

Inherently Safer Design and Optimization of Intensified Separation Processes for Furfural Production

G. Contreras-Zarazúa,[†] E. Sánchez-Ramírez,[†] J. A. Vázquez-Castillo,[‡] J. M. Ponce-Ortega,[§] M. Errico,^{||} A. A. Kiss,^{*,†,‡,#} and J. G. Segovia-Hernández[†]

[†]Department of Chemical Engineering University of Guanajuato, Noria Alta S/N, Guanajuato, Gto. 36000, Mexico

[‡]Faculty of Chemical Sciences, Autonomous University of Chihuahua, Circuito Universitario 8, Campus II, Chihuahua, Chihuahua 31125, Mexico

[§]Chemical Engineering Department, Universidad Michoacana de San Nicolás de Hidalgo, Morelia, Michoacán 58060, México

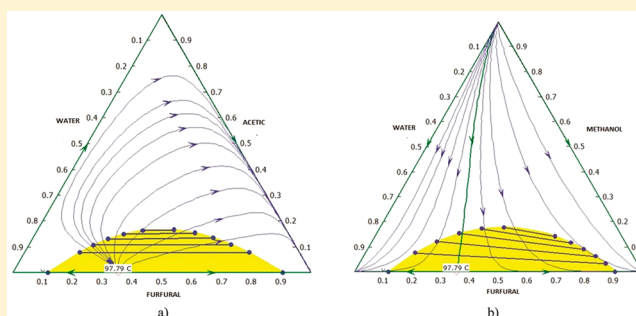
^{||}Department of Chemical Engineering, Biotechnology and Environmental Technology, University of Southern Denmark, Campusvej 55, DK-5230 Odense M, Denmark

[†]School of Chemical Engineering and Analytical Science, Centre for Process Integration, The University of Manchester, Sackville Street, The Mill, Manchester M13 9PL, United Kingdom

[#]Sustainable Process Technology, University of Twente, PO Box 217, 7500 AE Enschede, The Netherlands

Supporting Information

ABSTRACT: Currently furfural production has been the subject of increased interest because it is a biobased chemical able to compete with fossil-based chemicals. Furfural is characterized by flammability, explosion, and toxicity properties. Improper handling and process design can lead to catastrophic accidents. Hence it is of most importance to use inherent safety concepts during the design stage. This work is the first to present several new downstream separation processes for furfural purification, which are designed using an optimization approach that simultaneously considers safety criteria in addition to the total annual cost and the eco-indicator 99. The proposed schemes include thermally coupled configuration, thermodynamic equivalent configuration, dividing-wall column, and a heat integrated configuration. These are compared with the traditional separation process of furfural known as the Quaker Oats Process. The results show that because of a large amount of water present in the feed, similar values are obtained for total annual cost and eco-indicator 99 in all cases. Moreover, the topology of the processes has an important role in the safety criteria. The thermodynamic equivalent configuration resulted as the safest alternative with a 40% reduction of the inherent risk with respect to the Quaker Oats Process, and thus it is the safest option to purify furfural.



1. INTRODUCTION

The development of chemicals from renewable resources such as biomass attracted much research interest in recent years, with a focus on novel renewable building blocks such as furfural.¹ In fact, the U.S. Department of Energy compiled a list of Top 30 building block chemicals obtainable from biomass that could compete with chemicals derived from petroleum. Remarkably, furfural and two of its derivatives (furan dicarboxylic acid and levulinic acid) are highlighted in the top 10 in that list.^{2,3} Furfural has many industrial applications, being utilized as raw material for the production of other chemicals such as hexamethylenediamine (an intermediate compound used for the production of nylon-6-6)⁴ or phenol-furfural resins.⁵ Bhogeswararao and Srinivas⁶ proved that furfural can be converted to added-value chemicals such as furfuryl alcohol, tetrahydrofurfuryl alcohol, furan, tetrahydrofuran, and diols, using conventional Pt and Pd catalysts and

setting the appropriate reaction conditions and the support acidity. Because of its high affinity with molecules with double bonds, furfural is extensively used as an extractant.⁷ For example, Sun et al.⁸ and Cordeiro et al.⁹ have used furfural as solvent for the separation of a benzene/cyclohexane mixture in an extractive dividing-wall column arrangement.

Furfural is usually produced from biomass rich in pentosane, such as sugar cane bagasse, corncobs, oat hulls, and sunflower husks among others.^{1,7} In 1922, the Quaker Oats Company

Special Issue: Frameworks for Process Intensification and Modularization

Received: August 1, 2018

Revised: November 14, 2018

Accepted: November 19, 2018

Published: November 19, 2018

created the first process to produce furfural at the industrial scale using oat hulls as raw material, along with sulfuric acid and steam.⁷ This process has been characterized by easy implementation but a high purification cost and low conversions to furfural. The Quaker Oats process has not undergone great changes, and it is now used to produce near 80% of the total world production of furfural.^{7,10}

Up to now, most of the research work has focused on identifying cheap raw materials able to approach a sustainable and economic production of furfural. Blasi et al.¹¹ discussed the pyrolytic behavior of different hardwood and softwood biomasses with respect to the furfural yield. Mesa et al.¹² presented a study in which furfural is produced by diluted acid hydrolysis of sugar cane bagasse. De Jong and Marcotullio¹³ presented an overview of different technologies applied in various biorefineries where furfural is (co)produced. They also emphasize how diluted acid pretreatment can be beneficial for large-scale applications. Additionally, Martin and Grossman¹⁴ have proposed a process for the coproduction of furfural and dimethyl furfural from algae and switchgrass. Moreover, they explored different pretreatment technologies to improve the furfural conversion for many raw materials. Finally, Lui et al.,¹⁵ studied the possibility of taking advantage of hydrolysates of hardwoods to produce furfural.

However, there is a gap defining separation alternatives for product recovery leading to a strong interest in finding better downstream processing schemes in furfural production process. Typically, the solid biomass is treated with an acid solution at high temperature, and steam is used to maintain the reaction temperature and to remove the produced furfural obtained as a diluted aqueous stream. Similar to the separation of other bioderived compounds, such as bioethanol and biobutanol, the purification section represents one of the most energy-intensive parts of the process, and process intensification and optimization techniques are required to come up with innovative and competitive production processes.^{16–19} Distillation is usually the first unit operation considered for separation at industrial level due to the high reliability reached in modeling, simulation, design, and control, as well as the considerable amount of equilibrium data available.²⁰ However, due to its low thermodynamic efficiency and high capital investment it is imperative to define enhanced configurations based on process intensification principles,²¹ not considered at the time when the original process was developed.

Qian et al.²² proposed an azeotropic divided wall column to separate a mixture of water–furfural. Using the traditional two-column azeotropic configuration as a benchmark, the azeotropic divided wall alternative proposed provided 3.8% savings in the total reboiler duty and proved the applicability of traditional proportional–integral controllers. However, the feed chosen by the authors contained 90% mole of furfural which does not match with typical bioprocesses. Nhien et al.¹⁰ proposed a hybrid process in which furfural is recovered by liquid–liquid extraction. Many solvents were screened, but the best solution obtained was not compared against the traditional distillation alternative and its convenience was not proven. As an alternative to distillation, the application of pervaporation also has been proposed.²³

In this context, the definition of enhanced distillation configurations is of paramount importance in defining a furfural separation process integrated into a biorefinery. However, there are no previous studies that include safety criteria into the design of such a process. Medina-Herrera et

al.^{24,25} evaluated the inherent risk for distillation schemes with hydrocarbons mixtures and intensified extractives distillation schemes to recover ethanol. Their results indicate that the amount of inventory in the columns and the physical properties of the substances have a strong impact on the inherent safety of the process. Martinez-Gomez et al.²⁶ studied different intensified distillation processes to purify biobutanol and evaluated their individual risk—which is an index to evaluate the inherent safety—while considering economic and environmental criteria. Their results demonstrate that the process topology can influence the inherent safety. Additionally Martinez-Gomez et al.²⁷ carried out a safety analysis of a process to produce silane by reaction distillation—one of the most popular examples of process intensification. Their results show that process intensification can lead to important improvements in the safety aspects. On the previous studies, it is evident that process intensification can be a powerful tool to improve not only the economical and energy aspects but also the process safety.

This study is the first to propose four intensified distillation sequences for furfural purification, and compare them with the separation section included in the Quaker Oats process. These separation processes were designed and optimized simultaneously considering a multiobjective function to analyze the process performance. The objective function combines the *individual risk* (IR) as quantification of the potential risk of the process, *total annual cost* (TAC) as key economic indicator, and *Eco-indicator 99* (EI99) that quantifies the environmental impact. The simultaneous evaluation of economics, environmental impact, and inherent safety at the design stage represents an important improvement in selecting the optimal separation process route. The novelty of this work is represented by the new configurations proposed as well as the selection of the best alternative to purify furfural considering simultaneously the safety, economic, and environmental criteria.

2. SIMULATION APPROACH

Rigorous Aspen Plus simulations of the separation process (using the RADFRAC model) are coupled with an optimization algorithm programmed in Excel through a Visual Basic macro. To maintain the study general and extendible to the majority of furfural plants, the average composition reported by Zeitsch⁷ was considered. As Zeitsch stated: “all furfural reactors known so far produce a vapor stream consisting of more than 90% water, of up to 6% furfural, and of various by-products mainly methanol and acetic acid”.⁷ The feed compositions considered in this work is water 90 wt %, furfural 6 wt %, methanol 2 wt %, and acetic acid 2 wt %, a temperature of 353 K and pressure of 2 atm, these data were taken from the out stream of reactive zone reported by Zeitsch⁷ and Nhien et al.²⁸ The feed flow rate used is 105,000 kg/h according to the estimated global furfural demand reported by Nhien et al.²⁸ Note that this feed stream, represents an average flow rate according to the recent investments, for example the plant at Dominican Republic with an estimated production of 35 ton/year reported by Marcotullio.²⁹ Even though the feed stream is an important issue during the basic design, the synthesis methodology used in this work may be used on several scaled-up scenarios. For example, Errico et al.³⁰ reported economic and energy savings by 25% with a feed stream of 100 lbmol/h as a reference feed stream. On the other hand Errico et al.,³¹ with a larger

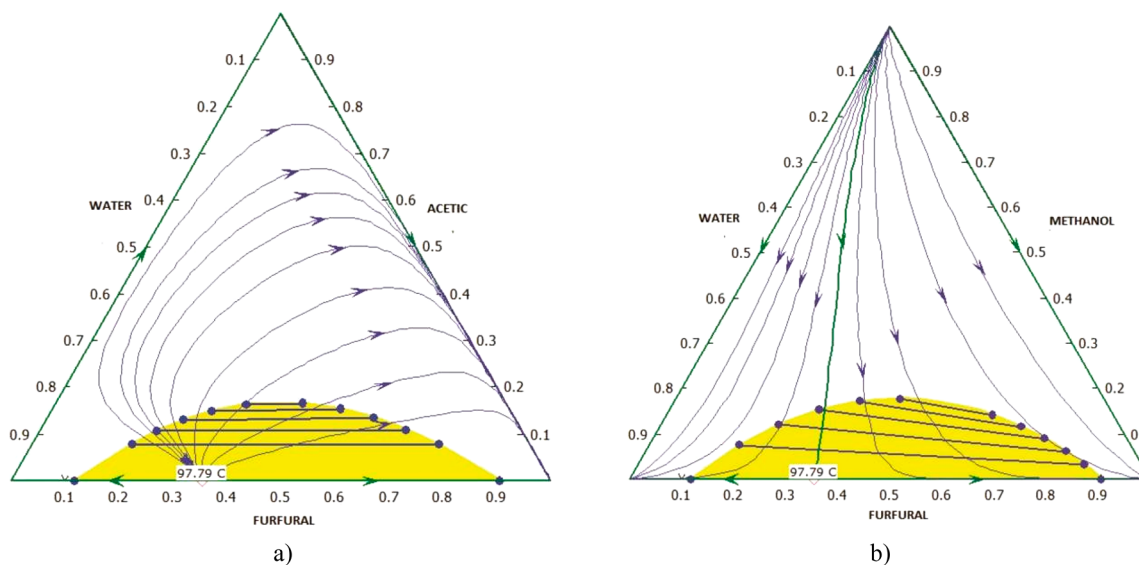


Figure 1. Ternary diagrams for mixtures: (a) water–furfural–acetic acid, (b) water–furfural–methanol.

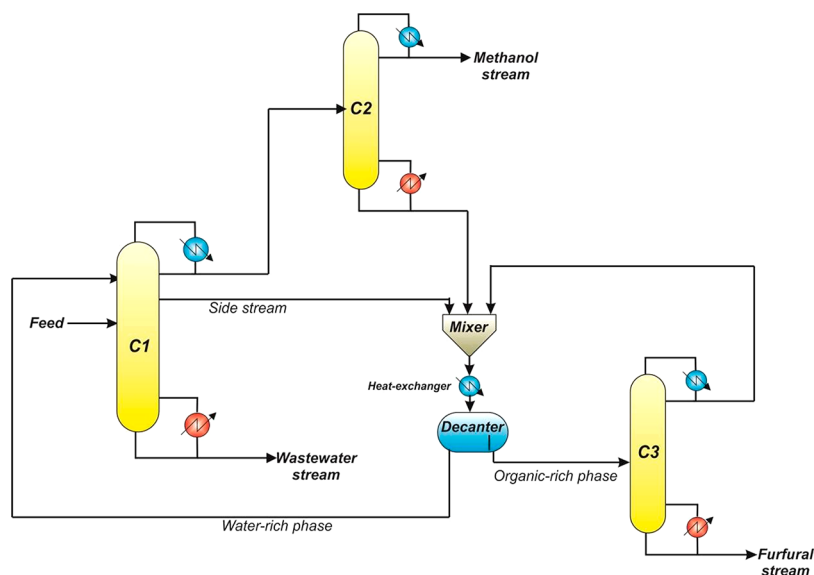


Figure 2. Benchmark configuration of the Quaker Oats Process.

production, also reported economic saving by 16%. The vapor–liquid–liquid equilibrium of this mixture can be adequately modeled using the property model nonrandom two-liquids with Hayden–O’Connell equation of state (NRTL-HOC) which takes into account the two liquid phases and the dimerization and solvation characteristics of mixtures with carboxylic acids.^{10,28} The NRTL-HOC model can also predict properly the heterogeneous azeotrope formed by water and furfural.^{10,28} The ternary diagrams for the ternary mixtures (using mass fraction as basis) are illustrated in Figure 1.

3. SYNTHESIS OF THE SEPARATION ALTERNATIVES

Figure 2 shows the classic furfural separation section considered as a benchmark. This configuration was developed according to the Quaker Oats Process (QOP), reported in detail by Zeitsch⁷ and Nhien et al.¹⁰ A similar configuration was also examined by Steingaszner et al.³² The benchmark configuration consists of three distillation columns and a decanter for the liquid–liquid separation. The first column

(C1) is commonly called an azeotropic distillation column. Within the C1 column, the mixture is concentrated until azeotrope composition. At this point, the water works as a very volatile component and dragging part of the furfural to the gas phase, which is condensate. After the condensation, two phases are formed and passed out to the decanter through the side stream. The phase enriched with water is returned to column C1 to promote the two liquids phases’ formation. Furthermore, the water is removed for the bottom of C1 together with the acetic acid, avoiding its probably expensive purification.⁸ The methanol is recovered as a distillate product of the second column (C2), while the bottom is fed to the decanter. The organic phase of the decanter is fed to the column C3 used for the final step of furfural recovery. The distillate of the column C3 is sent back to the decanter, while the bottom stream is the furfural product.

3.1. Thermally Coupled Separation Alternatives. Thermally coupled configurations are obtained from the corresponding simple column sequences by substitution of a

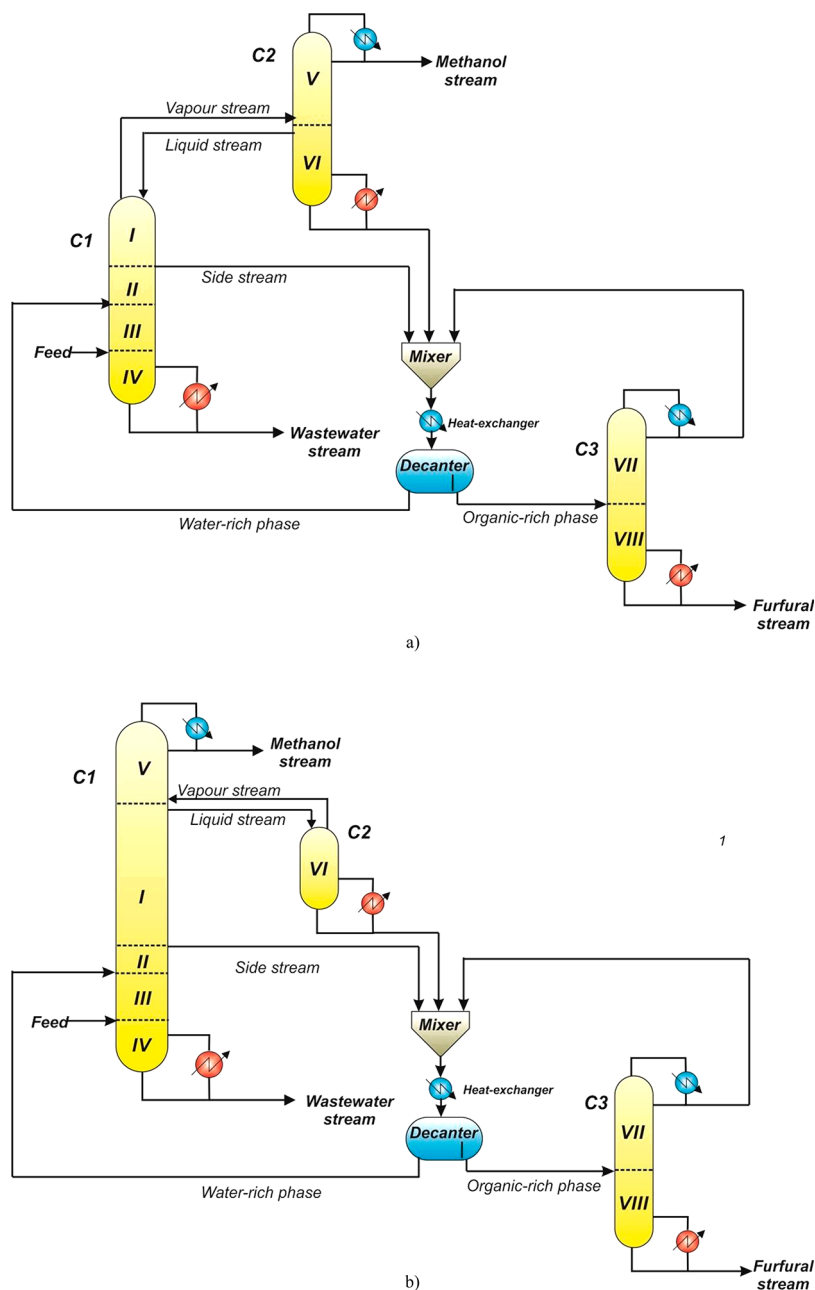


Figure 3. (a) Thermally coupled configuration (TCC); (b) thermodynamic equivalent configuration (TEC).

reboiler and/or a condenser not associated with product streams with a bidirectional liquid and vapor stream. The effect of the thermal coupling is related to the decrease of thermodynamic inefficiencies generated by the remixing of components. It was extensively proven that in many cases, thermally coupled configurations are more energy efficient as compared to simple column sequences.^{33–35} Starting from the reference configuration shown in Figure 2, it is possible to generate the thermally coupled arrangement; in this way the column is divided in sections, according to Hohmann et al.³⁶ a column section is commonly defined as a portion of distillation column not interrupted by entering or existing streams or heat flows. These sections are illustrated in Figure 3 with roman numerals. In the case of a thermally coupled configuration (TCC) shown in Figure 3a, the condenser associated with the first column was substituted by vapor and liquid streams which

are linked in the last and penultimate stages of section IV, respectively. This arrangement is commonly called thermal coupling. The introduction of this thermal coupling provides a flexibility to generate new designs, because the thermal coupling allows the sections between columns from a conceptual point of view. The corresponding thermodynamic equivalent configuration (TEC) is generated moving the section IV of the column C2 upon rectifying section I of column C1 as it is illustrated in Figure 3b. In general, for thermodynamic equivalent configurations, a better liquid and vapor flow rate redistribution among the column sections is expected together with a better controllability.^{37,38} For this reason, the TEC was considered as a possible alternative to the classic separation scheme.

3.2. Dividing-Wall Column Configuration. Dividing-wall columns are considered as a leading example of process

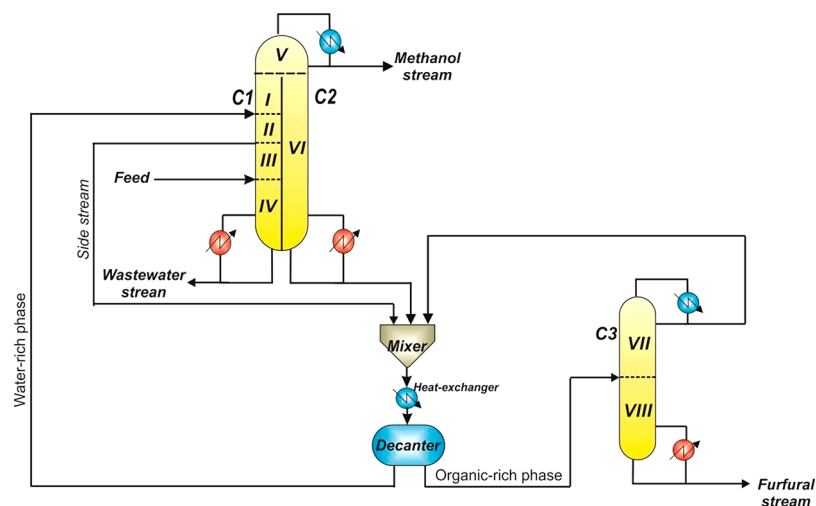


Figure 4. Dividing-wall column configuration (DWCC).

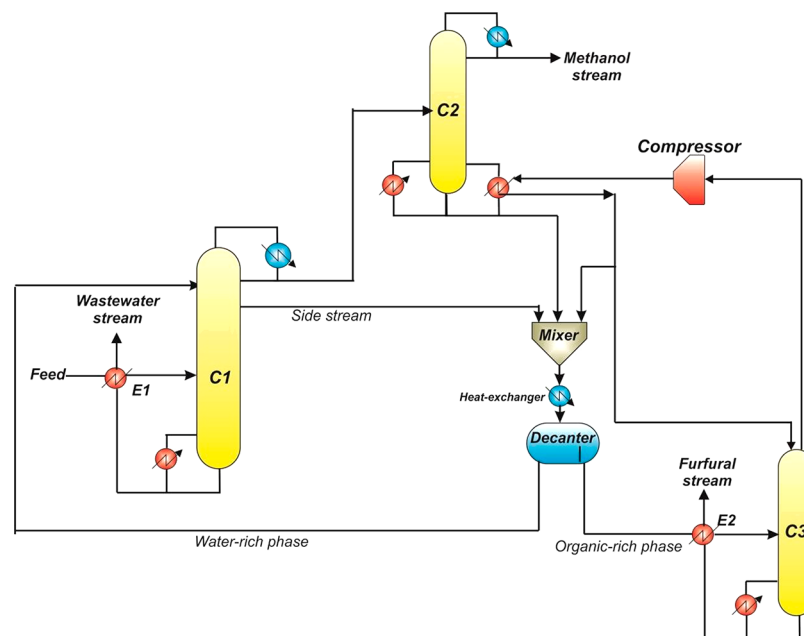


Figure 5. Heat integrated configuration (HIC).

intensification applied to multicomponent distillation. This configuration is an attractive alternative since it has the potential for reducing the operating and capital costs. Previous works explored among others the design and controllability of the dividing wall columns, and possible applications to the separation of biofuels.^{39–44} The divided wall column configuration (DWCC) considered for the furfural separation is shown in Figure 4. It was obtained merging column C1 and C2 in a single shell divided by an internal wall. From a conceptual point of view the length of the wall is determined by the number of trays of the sections of columns C1. The wall is extended to the column bottom in order to separate two bottom streams. For this reason, the DWCC unit is equipped with two reboilers. However, only one distillate product is obtained.

3.3. Heat Integrated Configuration. The main principle behind heat integration in distillation configurations is to use the energy sources or sinks available in other process streams to condense the vapor in the overhead of a column, or to

provide the reboiler duty required. As reported by Rathore et al.⁴⁵ the process streams might be the reboiler or condenser streams in the same separation sequence. Heat integrated alternatives were deeply explored in the literature, and they still represent a valid alternative to reduce the energy requirements of multicomponent distillation.^{45–51} The heat integrated configuration (HIC) considered in this work is illustrated in Figure 5. The selected heat integration strategy for the heat integrated configuration (HIC) consists of the utilization of the latent heat of the vapor stream leaving the top part of the column C3. The temperature of this stream is increased through the use of a compressor; the main target in this configuration with heat integration is to upgrade and reuse the heat of the vapor stream to mitigate the duty in the reboiler of C2 and to condensate the vapor. After condensation, it is partially recycled to the column C3 to ensure the liquid reflux. The function of the compressor is to increase the temperature of the vapor stream in order to guarantee that its temperature is higher than the temperature of the bottom of the column 2.

The heat integration can cause important energy savings in the process. This strategy has gained attention in recent years, and it has been proven to achieve an efficient method for heat integration in separation processes, for instance see the works by Jana and Maiti;⁴⁸ Luo et al;⁴⁹ Contreras Zarazúa et al.⁵⁰ and Zang et al.⁵¹

4. OBJECTIVE FUNCTION DEFINITION

The objective function is constructed by combining three different and contrasting indexes representing the economy (total annual cost), the environmental impact (eco-indicator 99), and the process safety (individual risk). Each index is described in the following subsections.

4.1. Plant Economy: Total Annual Cost (TAC). TAC is the classical approach used to quantify the economic performance of a chemical process alternative. The methodology consists in calculating the annualized cost of each processes equipment (capital cost) and the operating cost associated with the use of steam, cooling water, and electricity. The equation for TAC is given by

$$\text{TAC} = \frac{\text{capital cost}}{\text{payback period}} + \text{operating cost} \quad (1)$$

The capital cost includes the cost of condensers, reboilers, distillation columns, trays, process vessels and compressors, whereas the operating cost is associated with the cost of steam, cooling water, and electricity. The TAC was calculated using the Guthrie method.⁵² Carbon steel was considered as construction material. A payback period of 10 years was used. Sieve trays and 0.61 m spacing were selected for all the columns. All the parameters for the equipment and the utility costs were taken from Turton et al.⁵³ Five utility costs have been considered: high-pressure steam (42 bar, 254 °C, \$17.7/GJ), medium-pressure steam (11 bar, 184 °C, \$14.83/GJ), low-pressure steam (6 bar, 160 °C, \$14.95/GJ), cooling water (\$0.72/GJ), and electricity (\$16.8/GJ). The operating costs were evaluated considering 8500 h of yearly operation.

4.2. Environmental Impact: Eco-Indicator 99 (EI99). The EI99 was used to evaluate the sustainability of the processes and to quantify the environmental impact due to the multiple activities performed in the process. This methodology is based on the life cycle assessment. The approach was proposed by Goedkoop and Spriensma.⁵⁴ The EI99 has proven to be an important method to evaluate overall environmental impact related in chemical processes. Some authors, such as Guillen-Gonzalez et al.,⁵⁵ Alexander et al.,⁵⁶ and Quiroz-Ramirez et al.,⁵⁷ have demonstrated that applying the EI99 during the design and synthesis phases can lead to important improvements and reductions of wastes. The index was applied successfully in screening different alternatives for biofuels purification giving as results the optimal configuration with the lowest environmental impact and cost.^{19,30}

The method is based on the evaluation of three major damage categories: human health, ecosystem quality, and resources depletion. In the case of distillation columns, the factors that have the strongest influence on EI99 are the steam used to supply the heat duty, electricity utilized for pumping of cooling water, and the steel necessary to build the equipment.^{19,30} The EI99 can be represented mathematically according to the following equation:

$$\text{EI99} = \sum_i \omega c_i \text{as} + \sum_i \omega c_i \text{asl} + \sum_i \omega c_i \text{ael} \quad (2)$$

where ω is a weighting factor for damage, c_i is the value of impact for category i , “as” is the amount of steam utilized by the process, asl is the amount of steel used to build the equipment, and ael is the electricity required by the process. For example, the amount of steam used to provide energy to the plant is multiplied by the damage impact of each category, and subsequently the summation of all the products is performed to obtain the eco-indicator due to steam; the procedure is the same for steel and electricity. For the weighting factor ω , we have followed the method of EI99, separating the impact categories as damages to the human health (expressed in disability adjusted life years “DALYs”), damage to the ecosystem quality (expressed as the loss of species over a certain area% species m² yr), and damage to resources (expressed as the surplus energy needed for future extractions of minerals and fossil fuels, “MJ surplus”). The damage to the human health and to the ecosystem quality are considered to be equally important, whereas the damage to the resources is considered to be about half as important. Furthermore, in the presented approach the hierarchical perspective was considered to balance the short- and long-term effects. The normalization set is based on a damage calculation for all relevant emissions, extractions and land-uses.⁵⁸ Table 1 shows the values for the impact categories (c_i).

Table 1. Values of EI99 Impact Categories Used for Distillation Columns⁵⁴

impact category	steel (points/kg) $\times 10^{-3}$	steam (points/kg)	electricity (points/kWh)
carcinogenic	1.29×10^{-3}	1.180×10^{-4}	4.360×10^{-4}
climate change	1.31×10^{-2}	1.27×10^{-3}	4.07×10^{-3}
ionizing radiation	4.510×10^{-4}	1.91×10^{-6}	8.94×10^{-5}
ozone depletion	4.550×10^{-6}	7.78×10^{-7}	5.41×10^{-7}
respiratory effects	8.010×10^{-2}	1.56×10^{-3}	1.01×10^{-5}
acidification	2.710×10^{-3}	1.21×10^{-4}	9.88×10^{-4}
ecotoxicity	7.450×10^{-2}	2.85×10^{-4}	2.14×10^{-4}
land occupation	3.730×10^{-3}	8.60×10^{-5}	4.64×10^{-4}
fossil fuels	5.930×10^{-2}	1.24×10^{-2}	1.01×10^{-2}
mineral extraction	7.420×10^{-2}	8.87×10^{-6}	5.85×10^{-5}

Finally, the total EI99 is obtained by the summation of eco-indicators due to steam, electricity, and steel. To compute the EI99, a hierarchical perspective is considered for the evaluation of environmental impact in order to have a balance between short- and long-term effects.^{54,57} The values of Table 1 were taken from the work reported by Goedkoop and Spriensma⁵⁴ and are associated and corresponding with the use of steel for building the equipment and with the use of energy utilized during the plant operation, two factors that are independent of the type of process.

The scale of the values considered in Table 1 is chosen such that the value of 1 point is representative for a 1000th of the yearly environmental load of one average European inhabitant.^{30,54,55}

4.3. Process Safety: Individual risk (IR). The individual risk (IR) was used as index to evaluate the safety. The IR can be defined as the risk of injury or decease to a person in the

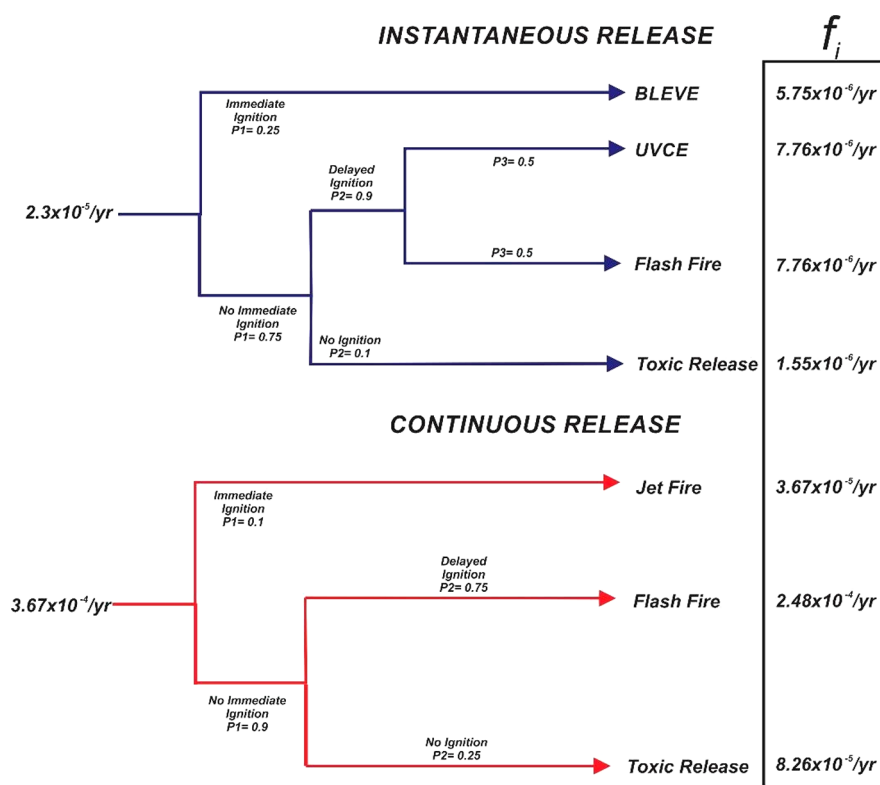


Figure 6. Event tree diagrams for distillation schemes^{59,24}

vicinity of a hazard.⁵⁹ The main objective of this index is the estimation of likelihood affectation caused by the specific incident that occurs with a certain frequency. The IR does not depend on the number of people exposed. The mathematical expression for calculating the individual risk is given in eq 3:

$$IR = \sum f_i P_{x,y} \quad (3)$$

Where f_i is the occurrence frequency of incident i , whereas $P_{x,y}$ is the probability of injury or decease caused by the incident i . In this work, an irreversible injury (decease) is used, for which more data are recorded. The calculation of IR can be carried out through quantitative risk analysis (QRA), which is a methodology used to identify incidents and accidents and their consequences. The QRA starts with the identification of possible incidents. Two types of incidents are identified for distillation columns: continuous and instantaneous releases. A continuous release is produced mainly by a rupture in a pipeline or partial rupture on process vessel causing a leak. The instantaneous release consists of the total loss of matter from the process equipment originated by a catastrophic rupture of the vessel. These incidents were determined through a hazard and operability study (HAZOP). The procedure is effective in identifying hazards and it is well accepted by the chemical industry. The technique consists of systematically analyzing the reasons and consequences that can provoke deviations in the operative conditions of a process that can derivate in an accident through a series of questions such as how, where, when, etc. More information about this technique is provided by AIChE⁵⁹ and Crowl and Louvar.⁶⁰ The frequency values for each incident (f_i) were taken according to those reported by American Institute of Chemical Engineers (AIChE).⁵⁹ Figure 6 shows the event tree diagrams obtained with all probabilities of instantaneous and continuous incidents, along with their

respective frequencies. Accordingly, instantaneous incidents are boiling liquid expanding vapor explosion (BLEVE), unconfined vapor cloud explosion (UVCE), flash fire, and toxic release, whereas the continuous release incidents are jet fire, flash fire and toxic release. The complete set of equations to calculate the IR is shown in the eqsS1–S8 of the [Supporting Information](#) and more information about these equations is given by AIChE⁵⁹ and Crowl and Louvar.⁶⁰

Once the incidents have been identified, the probability $P_{x,y}$ can be calculated through a consequence assessment, which consists of determining the physical variables such as the thermal radiation, the overpressure, and the concentration of the leak originated by incidents, and their respective damages. The calculation of the physical variables was realized according to the equations reported by the AIChE⁵⁹ and some other authors such as Medina-Herrera et al.^{24,25} The atmospheric stability type F is used for calculating the dispersion, which corresponds to a wind speed of 1.5 m/s. This atmospheric condition is the worst possible scenario because the the low wind speed does not allow a fast dispersion of the flammable and toxic components, increasing the time of exposure and the probability of contact with an ignition source.^{59,60}

The quantification of the damage caused by physical variables of each incident is calculated through a vulnerability model commonly known as a probit model.^{59,60} In this work, the damage considered to people is death due to fires, explosions, and toxic releases; all calculations were carried out to a representative distance of 50 m. The probit models associated with deaths by thermal radiation ($t_e E_r$) and overpressure due to explosions (p^0) are given by eq 4 and eq 5:⁵⁹

Table 2. Physical Properties of Components

component	lower flammability limit (LFL)	upper flammability limit (UFL)	lethal concentration (LC50)	heat combustion (kJ/mol)
furfural	2	19	64 000 ppm/4 h	2344
methanol	6	36	1037 ppm/1 h	726
acetic acid	6	17	16 000 ppm/4 h	876.1

$$Y = -14.9 + 2.56 \ln \left(\frac{t_e E_r^{\frac{3}{4}}}{10^4} \right) \quad (4)$$

$$Y = -77.1 + 6.91 \ln(p^\circ) \quad (5)$$

Because toxicity probit models for components considered in this work were not reported, the calculation of the damage to toxic releases were carried out using the LC50.⁵⁹ More information about this calculation is provide in the [Supporting Information](#). Finally, the probability $P_{x,y}$ is calculated substituting the probit results of eq 4 and eq 5 into the following equation:

$$P_{x,y} = 0.5 \left[1 + \operatorname{erf} \left(\frac{Y - 5}{\sqrt{2}} \right) \right] \quad (6)$$

The physical properties for each substance used for the consequence assessment are reported in Table 2. These were taken from the National Institute for Occupational Safety and Health (NIOSH).⁶¹

4.4. Multiobjective Optimization Problem Formulation. Once the economic, environmental, and safety indexes have been described, the mathematical optimization problem considering all indexes can be expressed according to

$$\begin{aligned} \min[\text{TAC}, \text{EI99}, \text{IR}] \\ = f(\text{NT}, \text{Fs}_i, \text{R}_i, \text{VF}, \text{LF}, \text{DC}_i, \text{HD}_i, k, \text{C}_{ij}) \end{aligned}$$

Subject to:

$$\begin{aligned} \vec{y}_m &\geq \vec{x}_m \\ \vec{w}_m &\geq \vec{u}_m \end{aligned} \quad (7)$$

where NT_i represents the total number of stages of column i , Fs_i is the feed stages for column i , R_i is the reflux ratio of column i , VF is the interconnection vapor flow, LF is the interconnection liquid flow, DC_i is the diameter of column i , HD_i is the reboiler duty for column i , k is the compressor capacity, C_{ij} is the concentration of substance j in column i . The optimization problem is restricted to satisfy the constraint vectors of purity and mass flow rate for interesting substances in the mixture. In this work y_m and w_m are the vectors of obtained purity and mass flow rate, while u_m and x_m are the vectors of required purity and mass flow rate, respectively. The purity constraints for methanol and furfural were defined as 99.5% and 99.2% mass fraction, whereas the mass flow rate was set at 2000 kg/h for methanol and 6200 kg/h for furfural in the methanol and furfural streams, respectively. Note that eq 7 is a general equation for all sequences, some terms such as interconnection flows, capacity of compressor, or heat duty for a specific column could be discarded depending on the studied scheme. Table 3 shows detailed information about the decision variables considered for each of the separation schemes. The letter “X” indicates that a particular process contains the discrete variable and continuous variable; e.g., the QOP process contains the number of stages of C1 as discrete

Table 3. Decision Variables of the Separation Process Configurations

decision variables	QOP	TCC	TEC	DWCC	HIC
Discrete Variables					
no. of stages, C1	X	X	X	X	X
no. of stages, C2	X	X	X	X	X
no. of stages, C3	X	X	X	X	X
feed stage recycle of C1	X	X	X	X	X
feed stage, C1	X	X	X	X	X
stage of side stream C1	X	X	X	X	X
feed stage C2	X	X	X	X	X
feed stage C3	X	X	X	X	X
Continuous Variables					
mass flow side stream C1	X	X	X	X	X
reflux ratio of C1	X	-	X	-	X
reflux ratio of C2	X	X	-	X	X
reflux ratio of C3	X	X	X	X	X
heat duty of C1, kW	X	X	X	X	X
heat duty of C2, kW	X	X	X	X	X
heat duty of C3, kW	X	X	X	X	X
diameter of C1, m	X	X	X	X	X
diameter of C2, m	X	X	X	X	X
diameter of C3, m	X	X	X	X	X
discharge pressure of compressor	-	-	-	-	X
interlinking flow	-	X	X	X	-
heat integrated E1, kW	-	-	-	-	X
heat integrated E2, kW	-	-	-	-	X
total number of variables	18	18	18	18	21

variable and the reflux ratio of C1 as continuous variable, then the “X” points out the existence of these variables in that process. On the other hand the “-” indicates the absence of either continuous or discrete variables in a process. Note in the QOP process the “-” indicates that this process configuration does not have a continuous variable called interlinking flow. The ranges of decision variables are reported in the Table S2 of [Supporting Information](#). The ranges for the design variables are within the limits reported by Gorak and Olujic.⁶²

4.5. Multiobjective Optimization Strategy. This study uses a multiobjective optimization technique known as Differential Evolution with Tabu List (DETL) proposed by Srinivas and Rangaiah,⁶³ which is a stochastic global optimization technique. The DETL algorithm combines two very useful optimization techniques, the differential evolution (DE) and Tabu search (TS). The differential evolution method is a population-based direct search method that imitates the biological evolution—it was designed to solve optimization problems with nonlinear and nondifferentiable equations.⁶⁴ The Tabu search is a random search method that has the ability to remember the search spaces previously visited.⁶³ The main advantages provided by DE is its faster convergence to the neighborhood global optimum in comparison to other stochastic methods; this algorithm has the capacity to escape from local due to its nature to be a method of global search. The main characteristic of TS is

avoiding revisiting the search space through the introduction of a so-called taboo list, leading to a reduction in the computational time.⁶³ The advantage of combining the DE with taboo list concept is a faster convergence to vicinity of global optima compared with a single differential evolution method and less computational time and effort.^{63,65} The implementation of the DETL method is carried out in a hybrid platform, which involves a link between Microsoft Excel and the process simulator Aspen Plus, where the optimization algorithm is programmed in Excel through a Visual Basic macro, whereas Aspen Plus is used to rigorously simulate the process. In general terms, all modules in the flowsheets of the cases of study were solved in Aspen by means of solving the entire set of MESH (material balances, equilibrium relationships, summation equations, and heat (enthalpy) balances). The DETL algorithm consists mainly of four steps which are initialization, mutation, crossover, and evaluation-selection.^{63,66} In general these steps are described as follows:

Initialization. In the initialization step the algorithm search in a D-dimensional space \mathcal{R}^D , where different vectors are generated randomly in a certain limited range of values (in this cases feasible diameters, reflux, trays of columns, etc.) for each different generation G. All these vectors are possible solutions for the optimization problem and can be represented according to eq 8.

$$\overrightarrow{X}_{i,G} = [X_{1,G}, X_{2,G}, X_{3,G}, \dots, X_{i,G}] \quad (8)$$

Mutation. The mutation step can be described as a change or disturbance occasioned by a random element (F). Starting from a parent vector (named target vector), this parent vector is further muted to generate a donor vector. Finally, the mutant vector is obtained recombining both the donor and target vector. We can write the process as eq 9

$$\overrightarrow{V}_{i,G} = \overrightarrow{X}_{r_1,G} + F(\overrightarrow{X}_{r_2,G} - \overrightarrow{X}_{r_3,G}) \quad (9)$$

Where $\overrightarrow{V}_{i,G}$ is the mutant vector, $\overrightarrow{X}_{r_1,G}$ is the parent vector, $\overrightarrow{X}_{r_2,G}$ and $\overrightarrow{X}_{r_3,G}$ are randomly vectors selected from the current generation, and F is the mutation factor.

Crossover. Following with the crossover step, the mutant vector exchanges its components with the target vector under this operation to form the trial vector $\overrightarrow{U}_{i,G} = [u_{1,i,G}, u_{2,i,G}, u_{3,i,G}, \dots, u_{D,i,G}]$. The cross is controlled by probability factor (Cr) which has values between 0 and 1. Each $u_{j,i,G}$ values of trial vector is generated by a randomly selection of values from mutant vector and parent vector according to eq 10.

$$u_{j,i,G} = \begin{cases} v_{j,i,G} & \text{if } (\text{rand}_{i,j}[0, 1]) \leq Cr \\ x_{j,i,G} & \text{otherwise} \end{cases} \quad (10)$$

where $\text{rand}_{i,j} [0,1]$ is an aleatory number, and $v_{j,i,G}$ and $x_{j,i,G}$ are elements from the mutant and parent vector, respectively.

Selection. Finally the evaluation-selection step is carry out to keep the population size as a constant number, the selection step determines if the target or the trial vector survives from the generation G to the next generation G + 1. The selection operation is described as follows in eq 11.

$$\begin{aligned} \overrightarrow{X}_{i,G+1} &= \overrightarrow{U}_{i,G} & \text{if } f(\overrightarrow{U}_{i,G}) \leq f(\overrightarrow{X}_{i,G}) \\ X_{i,G+1} &= X_{i,G} & \text{if } f(U_{i,G}) > f(X_{i,G}) \end{aligned} \quad (11)$$

The equation implies that if the trial vector $\overrightarrow{U}_{i,G}$ has a lower or equal value of objective function $f(\overrightarrow{X})$ than the target vector ($\overrightarrow{X}_{i,G}$), the trial vector replaces the corresponding target vector for the next generation. Both the Tabu list concept (TL) and Taboo Search (TS) previously proposed by Glover⁶⁷ avoids revisiting the search space by keeping a record of visited points. TL is randomly initialized at an initial population and is continuously updated with the newly generated trial individuals. This taboo check is carried out in the generation step to the trial vector, and the new trial individual is generated repeatedly until it is not near to any individual in the TL. The total trial individuals NPs are generated by the repetition of above steps. The newly generated NP trial vectors are combined with the parent population to form a combined population with total 2NP individuals.

During the optimization, a vector of decision variables (this vector can be the trial or target vector) is sent from Excel to Aspen Plus using Dynamic Data Exchange (DDE) through COM technology. Those values are used by Aspen Plus to simulate the process and obtain data as flow streams, purities, reboiler heat duty, etc., and these data are used for evaluate the objective function. After simulation, Aspen Plus returns to Microsoft Excel a resulting vector that contains the output data generated by Aspen. In the case that an Aspen simulation generated with trial vector values does not converge, the trial vector is automatically discarded. Then, Microsoft Excel analyzes the objective function values and new vectors of decision variables are generated according to the DETL method previously explained. The values of the required parameters to the DETL algorithm are the following: number of population (NP), 120 individuals; Generations Number (GenMax), 710; Tabu List size, 60 individuals; Tabu Radius, 0.01; Crossover fractions (Cr), 0.8; mutation fractions (F), 0.3. These values were taken from Srinivas and Rangaiah.^{63,66}

5. RESULTS AND DISCUSSION

This section presents the main results of the design and simultaneous optimization considering the economic, environmental, and safety criteria. The results obtained satisfy the constraints related to the purity (99.2 wt % for furfural and 99.5 wt % for methanol), whereas the mass flow rate was set to 6200 kg/h for furfural and 2000 kg/h for methanol. All sequences were optimized using RADFRAC module which is a rigorous model included in Aspen Plus. All optimizations were carried out on a computer with AMD Ryzen 5-1600 @3.2 GHz, and 16GB of RAM. The computing time for obtaining the optimal pareto solutions is different for each process separation according to the complexity: QOP required 278 h, TCC required 336 h, TEC required 328, DWCC required 350 h and HIC required 345 h.

The Pareto front charts are used to analyze in a simpler way the obtained results. The objective of this section is to identify the best option to purify furfural through the analysis of Pareto fronts and performance indexes of the processes. The points of the Pareto fronts correspond to the 120 individuals for the generation 710 (last generation). After this generation there are no more improvements in the objective functions, which means that the results obtained are the optimal solutions. Figures S1–S3 shows the evolution of Pareto front through the generations for the TEC process as a representative case, in order to demonstrate that the objective functions cannot be

further improved. The Pareto fronts are shown in two dimensions to simplify the analysis and the explanations of the results for a better understating.

Figure 7 shows the Pareto chart for the eco-indicator vs total annual cost. Each point in the plot represents a design for a

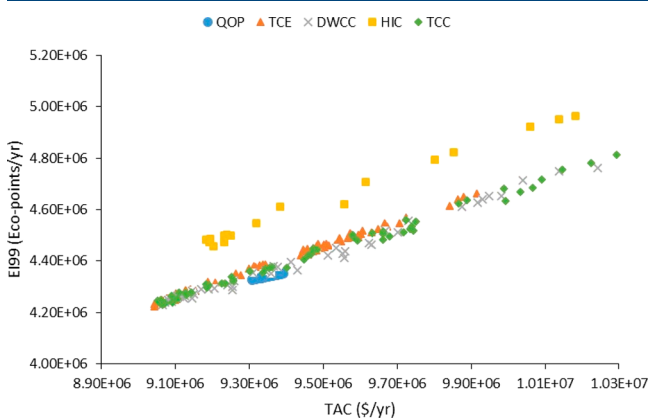


Figure 7. Pareto front between Eco-Indicator 99 and total annual cost.

respective process separation scheme. The designs to the right side of the graph are characterized by more stages, larger diameters, and higher energy usage. The form of the Pareto front indicates that the eco-indicator is strongly influenced by the steam used to supply the energy in the processes, and the electricity necessary to pump the cooling water, whereas the steel used for equipment exerts less influence. Previous works, as the one reported by Sanchez-Ramirez et al.,⁶⁵ have demonstrated that when steel has a strong influence in the eco-indicator, the relationship between TAC and EI99 corresponds to competing objectives. As can be noticed, there are several designs for all intensified schemes that have significant improvements in TAC and EI99 with the exception of heat integrated process (HIC) that has greater eco-indicator values than the benchmark configuration (Quaker Oats Process). This increment in the EI99 index is due to the extra equipment, such as the exchangers E1, E2, and the compressor required to integrate the heat between different streams.

Figure 8 shows the Pareto front of IR vs TAC. These indexes have a behavior of antagonist objectives, which means that it is not possible to obtain a design with the lowest TAC and IR at the same time, hence when an index improves the other one

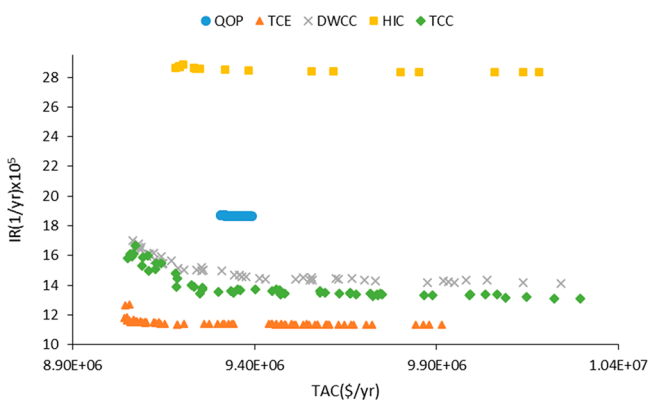


Figure 8. Pareto front between individual risk and total annual cost.

gets worse. The individual risk depends mainly on two things, the first one is the physical properties of the substances to be separated, for example, toxicity (LC50), flammability limits (LFL and UFL), and heat combustion, while the second one is the amount of each component inside the columns. When the substances in the mixture to be separated and the topology of the separation schemes are analyzed, it is evident that water is the component in the largest amount (90 wt % in the mixture) and it is removed in the first column (C1), indicating that this equipment will have the largest size (with respect to other columns) and more inventory (mass inside the columns) and thus contribute more to the safety index. If the reflux and reboiler duty are large in C1, there is an increase of water amount in the column yielding to a dilution of the organic components in this equipment and thus improving the safety index (decreasing the risk). However, larger reflux ratios and reboiler duties involve an increment on TAC caused by the increased use of utilities (steam and electricity). A similar behavior occurs in the columns C2 and C3. Considering these arguments, it should be noted that the behavior showed here between the individual risk and the total annual cost cannot be generalized to all mixtures.

Figure 9 shows the Pareto front of the eco-indicator and individual risk. EI99 has the same tendency as TAC, so a

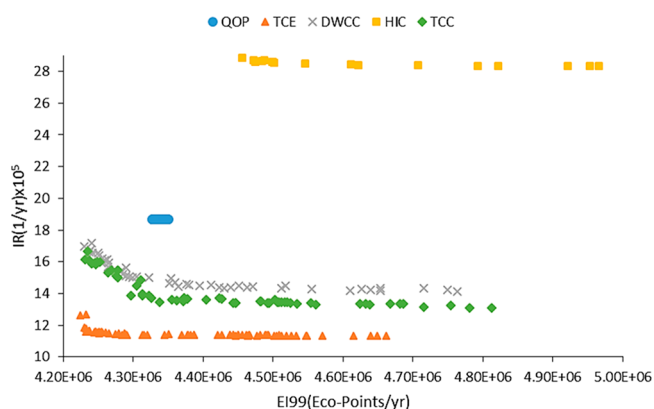


Figure 9. Pareto front between individual risk and Eco-Indicator 99.

similar behavior should be expected for both indexes. Here, major reflux ratios and reboiler duty imply higher use of steam and electricity, which impacts the eco-indicator. Because of the tendencies analyzed previously, it is clear that the designs chosen from the Pareto fronts should be those that have the best equilibrium between IR vs TAC and IR vs EI99. Because the eco-indicator and the total annual cost have the same tendency (see Figure 7), a design should be chosen that compensates the individual risk with TAC, for example, automatically selects the point with the best equilibrium between IR and EI99.

Figure 10, Figure 11, and Figure 12 show the Pareto charts of the thermodynamic equivalent sequence (TEC) as a representative case. It is important to mention that all these sequences have the same behavior for the Pareto fronts. The black points in these figures correspond to the design chosen for TEC, while similar points were selected for other separation sequences. The black triangles were selected according to the utopian point methodology. The utopic point corresponds to a hypothetical and ideal solution in the border of the Pareto front where two objectives cannot

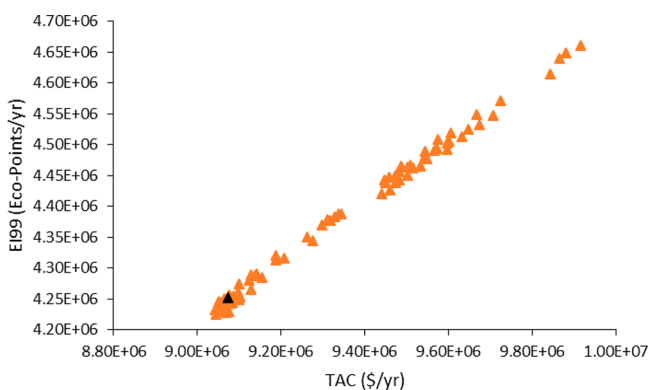


Figure 10. Pareto front between Eco-indicator 99 and total annual cost for TEC scheme.

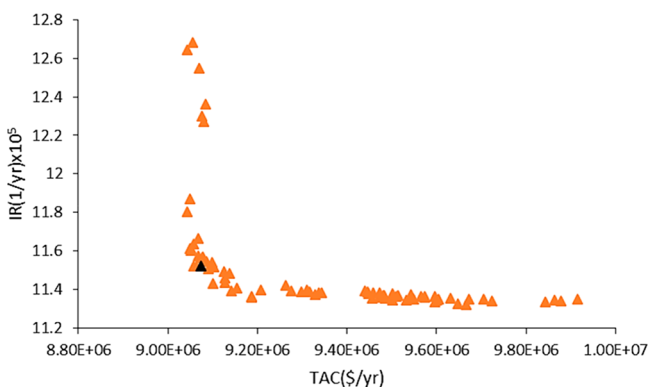


Figure 11. Pareto front between individual risk and total annual cost for TEC scheme.

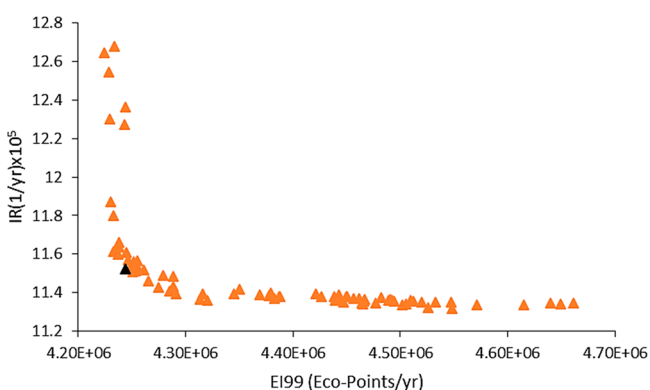


Figure 12. Pareto front between individual risk and Eco-Indicator 99 for the TEC scheme.

improve more and both are in equilibrium. The black triangles correspond to solutions closer to the utopic point according to a report by Wang and Rangaiah.⁶⁸ This methodology has been reported and implemented in several works by Contreras-Zarazua et al.,⁵⁰ Sanchez-Ramirez et al.,⁶⁵ Quiroz-Ramirez et al.,⁵⁷ and Medina-Herrera et al.²⁵ To demonstrate that the values of Pareto fronts are in the vicinity of the global optimum, the evolution of Pareto fronts through the generations for TEC sequences as a representative case is shown in the Figures S5–S7.

The optimal design parameters and values of the objective functions for all sequences are presented in Table 4. As can be observed on Table 4, the column C1 is the largest piece of

equipment from all schemes, which confirms the explanation previously mentioned: C1 is the column that contributes most to the three indexes. This column has the largest energy requirements and size, as it separates all water from the mixture. The energy required is very similar for all sequences, which leads to values of TAC and EI99 that are similar for all sequences. This can be demonstrated by observing the heat duty, the utilities cost, and the temperature of the C1 bottom given in Table 4.

The reflux ratio on C2 and C3 are small in order to reduce the concentration of methanol and furfural through the columns and thus to decrease the risk of an accident. The QOP scheme and all alternatives (with the exception of DWCC) show a clear tendency to reduce the number of stages in C2 and C3 in order to abate the quantity of methanol and furfural in the columns.

Commonly, the researchers considered that dividing wall columns offer important improvements in safety due to these configurations using fewer units with respect to thermally coupled configurations. However, this work demonstrated that dividing wall columns do not always represent the best option with respect to safety. The DWC is the integration of C1 and C2 columns in a single shell, which is showed in Figure 4. The stages and the diameter of C2 that purifies methanol need to increase in order to integrate the two columns, which causes an increase of the concentration and amount of methanol on the side corresponding to C2, and affecting directly the individual risk index. This situation does not occur in thermally coupled systems. Although DWCC is not the best alternative in terms of safety, it is an improvement compared with the QOP alternative. This improvement is caused mainly by the elimination of one condenser, and having a more diluted concentration of the organic substances.

The TCC and TEC sequences are in theory thermodynamic equivalents of DWC. However, the topology of the scheme has an important role in safety. TCC and TEC have lower IR than DWCC as the size of the C2 column is smaller than in the DWC configuration, thus reducing the inventory. TEC has the best IR results showing a reduction of almost 40% of the inherent risk as compared with QOP. This reduction occurs because methanol is purified in column C1 which is rich in water, thus reducing the methanol concentration and its toxic and flammability properties, while the C2 column does not purify methanol. The C2 column contains mainly water that is purified and sent to the decanter to promote the two liquid phase formation. The heat integrated configuration (HIC) shows the smallest energy consumption in column C1; however, the additional units (exchangers E1, E2 and compressor) offset the energy saving which is not reflected in TAC and EI99. In the case of the individual risk, these additional units imply higher chances of a leak, affecting directly the safety index.

According to the results it is evident that the TEC is the best option to purify furfural, it has similar total annual cost and eco-indicator compared with the other alternatives. Nevertheless, the topology of TEC process provides a greater dilution on the organic substances which improves the safety of process. Figure 13 shows a scheme of TEC process including all mass flows and energy requirements. Table 4 summarizes the optimal design parameters for all sequences considered. The best designs were selected according to utopian point methodology. The optimal design (the black triangle in Pareto

Table 4. Optimal Design Parameters for All Separation Sequences

design variables	QOP	TCC	TEC	DWCC	HIC
Columns Topology					
no. of stages, C1	55	91	97	81	61
no. of stages, C2	12	40	27	83	30
no. of stages, C3	6	11	9	11	7
feed stage of water-rich phase C1	22	14	26	6	24
feed stage, C1	27	54	65	39	33
stage of side stream C1	16	39	43	33	12
feed stage C2	8	16	1		27
feed stage C3	3	6	3	4	3
diameter of C1, m	0.44	1.1	1.02		0.71
diameter of C2, m	0.42	0.95	0.36	2.57	0.90
diameter of C3, m	1.63	1.67	0.8	1.23	1.4
Operation Specifications					
top pressure (atm)	1	1	1	1	1
reflux ratio of C1	18.5		24.5		6.2
reflux ratio of C2	0.21	25.24		25.14	0.83
reflux ratio of C3	0.208	0.265	0.455	0.233	3.82
heat duty of C1 (kW)	19 096.8	19 235	19 093	19 143	18 659
heat duty of C2 (kW)	770.17	117.1	76.5	191.2	1186.1
heat duty of C3 (kW)	456	1102	804.3	826.11	638
energy of compressor (kW)					12
total energy consumed (kW)	20 322.97	20 454	19 973.32	20 160.11	20 495.19
discharge pressure of compressor(Comp) (atm)					1.265
temp bottom C1 (°C)	100.09	100.01	100.09	100.09	100.07
temp bottom C2 (°C)	64.54	90.95	92.45	92.81	76.45
temp bottom C3 (°C)	143.43	161.4	146.39	154.05	161.38
Streams Mass Flow ((kg h ⁻¹))					
feed	105 000	105 000	105 000	105 000	105 000
methanol stream	2097.02	2102.2	2101	2099	2107.1
furfural stream	6308.37	6299.59	6304	6300.8	6263.2
waste water stream	96 594.7	96 599.6	96 597.5	96 602.2	96 629
side stream	23 293	23 712.9	70 008.4	22 931.8	26 580
water-rich phase stream	17 483	51 118.8	86 131.8	48 628.3	24 183.4
organic-rich phase stream	6584.2	8375.9	7464.96	7687.22	7591.3
liquid stream		3649.2	22 603.8	4696	
vapor stream		39456	179.8	38 790.3	
Purity of Main Components (Mass Fraction)					
methanol	0.9999	0.9999	0.9999	0.9999	0.9972
furfural	0.9924	0.9999	0.9938	0.9970	0.9999
Performance Index					
utilities cost (million\$/yr)	9.103	9.0243	8.8155	8.8972	9.1464
equipment cost (million\$)	2.307	2.7712	2.5965	3.5795	2.3791
TAC (\$/yr)	9.334	9.301	9.075	9.255	9.384
Eco99 (million Eco-points/yr)	4.335	4.3623	4.2555	4.2992	4.6118
IR (1/yr)×10 ⁵	18.674	13.548	11.516	12.302	28.450

front) corresponds to solutions closer to the utopic point according to a report by Wang and Rangaiah.⁶⁸

Even though all alternatives solve the MESH equations, both are also quite different. For example, internal-flows in the thermal couplings of TCC is not necessarily the same of the TEC. Moreover, the reflux ratio provided for section V in both cases is not the same, so evidently the MESH equations are not solved with the same parameter values. They are thermodynamically equivalent since they perform a similar task with a similar amount of energy, but structurally they are not equal. Regarding DWC, it is true that this alternative also carried out the same operation with similar energy; however, since the process unit possesses a single shell, the diameter values are not precisely the same.

An interesting work that shows a similar situation is the work of Hernández et al.⁶⁹ They propose a set of ternary dividing wall columns, presented in the way of Petlyuk columns. All the alternatives were generated by moving sections. In brief they proposed a set of six alternatives, and the thermodynamic efficiency was further calculated. Their results showed similar efficiencies; however, also the differences on the topology of all alternatives was clear. Although this work does not propose so many alternatives, the topologic differences of furfural alternatives may be understood under the light of the work of Hernández et al.⁶⁹

On the other hand, the industrial application of the Petlyuk column is the DWC. Note in the Aspen Plus simulator, the DWC must be simulated as a Petlyuk column; however, they

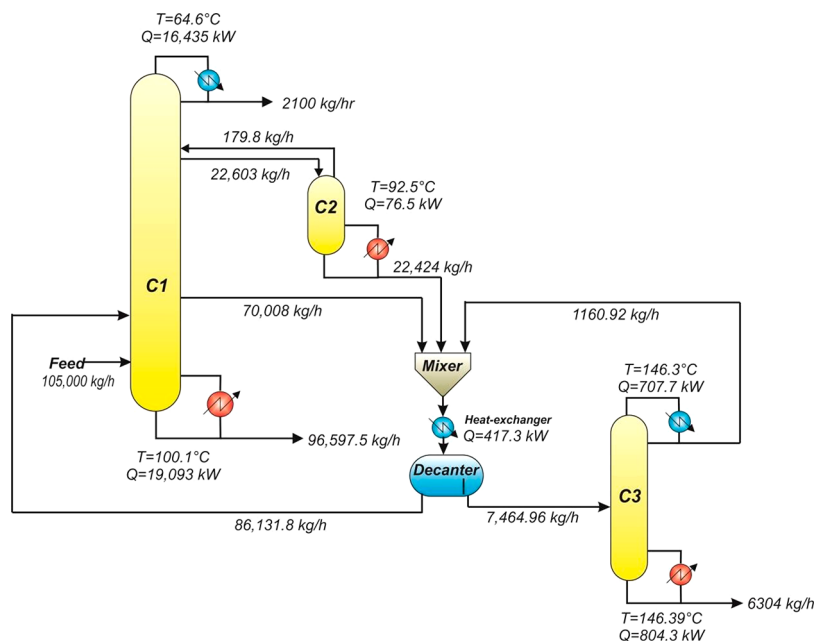


Figure 13. Mass flows and energy requirements for TEC process.

are different since several physical/sizing considerations must be taken into account. A wider explanation of the industrial implementation is provided by Yildirim et al.⁷⁰ Essentially, they perform the same task with the same amount of energy. In other words, they might be thermodynamically equivalent; however, they are structurally different.

6. CONCLUSIONS

The new downstream processing configurations (for furfural purification) proposed in this study are competitive against the Quaker Oats Process used as a benchmark. The schemes proposed in this work are azeotropic distillation systems and they correspond to the category of heterogeneous azeotropic distillations. These heterogeneous azeotropic schemes are formed with at least two columns. The heterogeneous azeotropic scheme can or cannot contain the use of entrainer depending of components in the mixture to be separated and their respective compositions. In this case, the water has the function of an entrainer because it is present in high concentration in the mixture. According to previous works (Widagdo and Seider, 1996) an azeotropic distillation column (azeotropic column) is the equipment that concentrates the mixture up to the azeotrope concentration.⁷¹ Then, the distillate or a side stream is condensed and sent to a decanter where one of the phases is refluxed to the column. The other phase is sent (organic phase in this case) to a second column where its purification is finalized. Finally the products in these two column systems are recovered by the bottoms of the columns. All alternatives were optimized using a DETL algorithm and considered the total annual cost, Eco-Indicator 99, and individual risk as key performance indexes. The results show that TAC and EI99 remain constant for all sequences. This occurs because column C1—the unit that contributes most to these indexes—uses most of the total energy of the sequences for the separation of the bulk water present in the mixture (90 wt %). This makes it difficult to improve the energy usage, TAC, and EI99 in all cases considered. However, the optimization results show that the topology of the

intensified separation schemes has an important role on the safety criteria which can be significantly improved by process intensification.

Compared to the QOP benchmark, the intensified thermally coupled sequences (TCC, TEC, and DWCC) exhibit major reductions (from 27% up to 40%) of the inherent risk associated with the lower concentration and amount of organic substances inside the distillation columns. For example, as the TEC process separates methanol and water in the same column, this leads to a dilution of methanol in the water which reduces their toxicity and flammability. However, the heat integrated configuration has the worst values of the inherent risk (52% higher IR) as this process implies the use of extra units and a compressor, which further increases the risks. Among all sequences, the intensified TEC alternative is overall the best option to purify furfural, being the significantly safer (about 40% lower IR) and slightly cheaper and more eco-friendly as compared with the QOP benchmark.

As has been discussed, the topology of the alternatives of this work are different. Even though the energy requirements are similar (thermodynamic equivalents) their structure is different. With this in mind, the differences associated with the IR values are understandable. However, the necessity (as future work) to know the layout of the process for better understanding of the distance among columns of the same process, and the role of that distance on IR calculation, is clear.

■ ASSOCIATED CONTENT

📄 Supporting Information

The Supporting Information is available free of charge on the ACS Publications website at DOI: 10.1021/acs.iecr.8b03646.

Continuous and instantaneous source models; dispersion models; boiling liquid expanding vapor explosion (BLEVE) model; flash fire model; toxic releases; additional figures (PDF)

AUTHOR INFORMATION

Corresponding Author

*E-mail: tony.kiss@manchester.ac.uk

ORCID

E. Sánchez-Ramírez: 0000-0002-4326-4837

J. M. Ponce-Ortega: 0000-0002-3375-0284

M. Errico: 0000-0002-2172-2921

J. G. Segovia-Hernández: 0000-0003-4175-9809

Notes

The authors declare no competing financial interest.

ACKNOWLEDGMENTS

A.A.K. gratefully acknowledges the Royal Society Wolfson Research Merit Award.

NOMENCLATURE

IR = individual risk
 TAC = total annual cost
 EI99 = Eco-Indicator 99
 QOP = Quaker Oats Process
 TCC = thermally coupled configuration
 TEC = thermodynamic equivalent configuration
 DWCC = dividing-wall column configuration
 HIC = heat integrated configuration
 C1 = column 1 (azeotropic column)
 C2 = column 2 (methanol recovery column)
 C3 = column 3 (furfural recovery column)
 ω = weighting factor for damage
 c_i = value of impact for category i
 as = amount of steam utilized by the process
 asl = amount of steel used to build the equipment
 ael = amount of electricity utilized by the process
 f_i = occurrence frequency of incident i
 P_{xy} = probability of injury or decrease caused by the incident i
 BLEVE = boiling liquid expanding vapor explosion
 UVCE = unconfined vapor cloud explosion
 t_{err} = thermal radiation doses
 p° = overpressure due to explosions
 Y = probit variable
 erf = error function
 LC50 = lethal concentration
 LFL = lower flammability limit
 UFL = upper flammability limit
 NT_i = total number of stages of column i
 Fs_i = feed stages for column i
 R_i = reflux ratio of column i
 VF = interconnection vapor flow
 LF = interconnection liquid flow
 DC_i = diameter of column i
 HD_i = reboiler duty for column i
 k = compressor capacity
 $C_{ij} = C_{ij}$ in the concentration of substance j in column i
 y_m = purity obtained during the simulation
 w_m = mass obtained during the simulation
 u_m = purity required
 x_m = mass flow required
 DETL = differential evolution with Tabu list
 TS = Tabu search
 DE = differential evolution
 G = number of generations

$\vec{V}_{i,G}$ = mutant vector

$\vec{X}_{j,i,G}$ = randomly vectors from the generation G

$\vec{U}_{i,G}$ = trial vector

$u_{j,i,G}$ = elements of the trial vector

$\vec{X}_{i,G+1}$ = parent vector of generation G + 1

NP = number of population

GenMax = maximum generation number

Cr = crossover fraction

F = mutation factor

REFERENCES

- (1) Steinbach, D.; Kruse, A.; Sauer, J. Pretreatment technologies of lignocellulosic biomass in water in view of furfural and 5-hydroxymethylfurfural production - A review. *Biomass Convers. Biorefin.* **2017**, *7* (2), 247–274.
- (2) Top value added chemicals from biomass volume I-Results of screening for potential candidates from sugars and synthesis gas; U.S. Department of Energy: 2004; <https://www.nrel.gov/docs/fy04osti/35523.pdf>.
- (3) Cai, C. M.; Zhang, T.; Kumar, R.; Wyman, C. E. Integrated furfural production as a renewable fuel and chemical platform from lignocellulosic biomass. *J. Chem. Technol. Biotechnol.* **2014**, *89* (1), 2–10.
- (4) Dros, A. B.; Larue, O.; Reimond, A.; De Campo, E.; Pera-Titus, M. Hexamethylenediamine (HDMA) from fossil- vs. bio-based routes: an economic and life cycle assessment comparative study. *Green Chem.* **2015**, *17*, 4760–4772.
- (5) Brown, L. H.; Watson, D. D. Phenol-furfural resins. *Ind. Eng. Chem.* **1959**, *51* (5), 683–684.
- (6) Bhogeswararao, S.; Srinivas, D. Catalytic conversion of furfural to industrial chemicals over supported Pt and Pd catalysts. *J. Catal.* **2015**, *327*, 65–77.
- (7) Zeitsch, K. J.; *The Chemistry and Technology of Furfural and Its Many by-Products*; Elsevier Science: Amsterdam, 2000.
- (8) Sun, L.; Wang, Q.; Li, L.; Zhai, J.; Liu, Y. Design and control of extractive dividing wall column for separating benzene/cyclohexane mixtures. *Ind. Eng. Chem. Res.* **2014**, *53*, 8120–8131.
- (9) Cordeiro, G. M.; de Figueiredo, M. F.; Ramos, W. B.; Sales, F. A.; Brito, K. B.; Brito, R. P. Systematic strategy for obtaining a divided-wall column applied to an extractive distillation process. *Ind. Eng. Chem. Res.* **2017**, *56*, 4083–4094.
- (10) Nhien, L. C.; Van Duc Long, N.; Lee, M. Process design of hybrid extraction and distillation processes through a systematic solvent selection for furfural production. *Energy Procedia* **2017**, *105*, 1084–1089.
- (11) Di Blasi, C.; Branca, C.; Galgano, A. Biomass screening for the production of furfural via thermal decomposition. *Ind. Eng. Chem. Res.* **2010**, *49*, 2658–2671.
- (12) Mesa, L.; Morales, M.; Gonzales, E.; Cara, C.; Romero, I.; Castro, E.; Mussatto, S. I. Restructuring the process for furfural and xylose production from sugarcane bagasse in a biorefinery concept for ethanol production. *Chem. Eng. Process.* **2014**, *85*, 196–202.
- (13) De Jong, W.; Marcotullio, G. Overview of biorefineries based on co-production of furfural, existing concepts and novel developments. *Int. J. Chem. React. Eng.* **2010**, *8* (1), A69 DOI: [10.2202/1542-6580.2174](https://doi.org/10.2202/1542-6580.2174).
- (14) Martín, M.; Grossmann, I. E. Optimal production of furfural and DMF from algae and switchgrass. *Ind. Eng. Chem. Res.* **2016**, *55* (12), 3192–3202.
- (15) Liu, L.; Chang, H. M.; Jameel, H.; Park, S. Furfural production from biomass pretreatment hydrolysate using vapor-releasing reactor system. *Bioresour. Technol.* **2018**, *252*, 165–171.
- (16) Errico, M.; Ramirez-Marquez, C.; Torres-Ortega, C. E.; Rong, B.-G.; Segovia-Hernandez, J. G. Design and control of an alternative distillation sequence for bioethanol purification. *J. Chem. Technol. Biotechnol.* **2015**, *90* (12), 2180–2185.

- (17) Luo, H.; Bildea, C. S.; Kiss, A. A. Novel heat-pump-assisted extractive distillation for bioethanol purification. *Ind. Eng. Chem. Res.* **2015**, *54*, 2208–2213.
- (18) Patrascu, I.; Bildea, C. S.; Kiss, A. A. Eco-efficient downstream processing of biobutanol by enhanced process intensification and integration. *ACS Sustainable Chem. Eng.* **2018**, *6*, S452–S461.
- (19) Errico, M.; Sanchez-Ramirez, E.; Quiroz-Ramirez, J. J.; Rong, B.-G.; Segovia-Hernandez, J. G. Multi objective optimal acetone-butanol-ethanol (ABE) separation systems using liquid-liquid extraction assisted divided wall columns. *Ind. Eng. Chem. Res.* **2017**, *56*, 11575–11583.
- (20) Kiss, A. A.; *Advanced distillation technologies - Design, control and applications*; Wiley: Hoboken, US, 2013.
- (21) Kiss, A. A. Distillation technology - Still young and full of breakthrough opportunities. *J. Chem. Technol. Biotechnol.* **2014**, *89*, 479–498.
- (22) Qian, X.; Jia, S.; Skogestad, S.; Yuan, X. Design and control of azeotropic dividing wall column for separating furfural-water mixture. *Comput.-Aided Chem. Eng.* **2016**, *38*, 409–414.
- (23) Ghosh, U. K.; Pradhan, N. C.; Adhikari, B. Pervaporative separation of furfural from aqueous solution using modified polyurethane membrane. *Desalination* **2010**, *252*, 1–7.
- (24) Medina-Herrera, N.; Jiménez-Gutiérrez, A.; Mannan, M. S. Development of inherently safer distillation systems. *J. Loss Prev. Process Ind.* **2014**, *29*, 225–239.
- (25) Medina-Herrera, N.; Grossmann, I. E.; Mannan, M. S.; Jiménez-Gutiérrez, A. An approach for solvent selection in extractive distillation systems including safety considerations. *Ind. Eng. Chem. Res.* **2014**, *53* (30), 12023–12031.
- (26) Martínez-Gómez, J.; Sánchez-Ramírez, E.; Quiroz-Ramírez, J. J.; Segovia-Hernández, J. G.; Ponce-Ortega, J. M.; El-Halwagi, M. M. Involving economic, environmental and safety issues in the optimal purification of biobutanol. *Process Saf. Environ. Prot.* **2016**, *103*, 365–376.
- (27) Martínez-Gómez, J.; Ramírez-Márquez, C.; Alcántara-Ávila, J. R.; Segovia-Hernández, J. G.; Ponce-Ortega, J. M. Intensification for the silane production involving economic and safety objectives. *Ind. Eng. Chem. Res.* **2017**, *56* (1), 261–269.
- (28) Nhien, L. C.; Van Duc Long, N.; Kim, S.; Lee, M. Design and optimization of intensified biorefinery process for furfural production through a systematic procedure. *Biochem. Eng. J.* **2016**, *116*, 166–175.
- (29) Marcotullio, Gianluca. *The chemistry and technology of furfural production in modern lignocellulose- feedstock biorefineries*. Ph.D. Dissertation, TU Delft, 2011.
- (30) Errico, M.; Sanchez-Ramirez, E.; Quiroz-Ramirez, J. J.; Segovia-Hernandez, J. G.; Rong, B.-G. Synthesis and design of new hybrid configurations for biobutanol purification. *Comput. Chem. Eng.* **2016**, *84*, 482–492.
- (31) Errico, M.; Rong, B. G. Synthesis of new separation processes for bioethanol production by extractive distillation. *Sep. Purif. Technol.* **2012**, *96*, 58–67.
- (32) Steingaszner, P.; Balint, A.; Kojnok, M. Improvement of a furfural distillation plant. *Period. Polytech. Chem. Eng.* **1977**, *21* (1), 59–71.
- (33) Rong, B.-G.; Kraslawski, A.; Nystrom, L. The synthesis of thermally coupled distillation flowsheets for separations of five-component mixtures. *Comput. Chem. Eng.* **2000**, *24*, 247–252.
- (34) Calzon-McConville, C. J.; Rosales-Zamora, Ma. B.; Segovia-Hernandez, J. G.; Hernandez, S.; Rico-Ramirez, V. Design and optimization of thermally coupled distillation schemes for the separation of multicomponent mixtures. *Ind. Eng. Chem. Res.* **2006**, *45*, 724–732.
- (35) Errico, M.; Rong, B.-G.; Tola, G.; Turunen, I. Process intensification for the retrofit of a multicomponent distillation plant - An industrial case study. *Ind. Eng. Chem. Res.* **2008**, *47*, 1975–1980.
- (36) Hohmann, E. G.; Sander, M. T.; Dunford, H. 1982. A new approach to the synthesis of multicomponent separation schemes. *Chem. Eng. Commun.* **1982**, *17* (1–6), 273–284.
- (37) Segovia-Hernández, J. G.; Hernández, S.; Rico-Ramírez, V.; Jiménez, A. A comparison of the feedback control behavior between thermally coupled and conventional distillation schemes. *Comput. Chem. Eng.* **2004**, *28* (5), 811–819.
- (38) Segovia-Hernández, J. G.; Hernández-Vargas, E. A.; Márquez-Munoz, J. A. Control properties of thermally coupled distillation sequences for different operating conditions. *Comput. Chem. Eng.* **2007**, *31* (7), 867–87.
- (39) Dejanović, I.; Matijašević, Lj.; Olujić, Ž. Dividing wall column - A breakthrough towards sustainable distilling. *Chem. Eng. Process.* **2010**, *49* (6), 559–580.
- (40) Gómez-Castro, F. I.; Segovia-Hernández, J. G.; Hernández, S.; Gutiérrez-Antonio, C.; Briones-Ramírez, A. Dividing wall distillation columns: Optimization and control properties. *Chem. Eng. Technol.* **2008**, *31* (9), 1246–1260.
- (41) Kiss, A. A. Novel applications of dividing-wall column technology to biofuel production processes. *J. Chem. Technol. Biotechnol.* **2013**, *88*, 1387–1404.
- (42) Patrascu, I.; Bildea, C. S.; Kiss, A. A. Dynamics and control of a heat pump assisted extractive dividing-wall column for bioethanol dehydration. *Chem. Eng. Res. Des.* **2017**, *119*, 66–74.
- (43) Errico, M.; Sanchez-Ramirez, E.; Quiroz-Ramirez, J. J.; Rong, B.-G.; Segovia-Hernandez, J. G. Biobutanol purification by hybrid extraction-divided wall column configurations. *Comput.-Aided Chem. Eng.* **2017**, *40*, 1027–1032.
- (44) Errico, M.; Rong, B.-G.; Tola, G.; Spano, M. Optimal synthesis of distillation systems for bioethanol separation. Part 2: Extractive distillation with complex columns. *Ind. Eng. Chem. Res.* **2013**, *52*, 1620–1626.
- (45) Rathore, R. N. S.; van Wormer, K. A.; Powers, G. J. Synthesis strategies for multicomponent separation systems with energy integration. *AIChE J.* **1974**, *20* (3), 491–502.
- (46) Alcántara-Avila, J. R.; Gómez-Castro, F. I.; Segovia-Hernández, J. G.; Sotowa, K. I.; Horikawa, T. Optimal design of cryogenic distillation columns with side heat pumps for the propylene/propane separation. *Chem. Eng. Process.* **2014**, *82*, 112–122.
- (47) Shi, L.; Huang, K.; Wang, S. J.; Yu, J.; Yuan, Y.; Chen, H.; Wong, D. S. Application of vapor recompression to heterogeneous azeotropic dividing-wall distillation columns. *Ind. Eng. Chem. Res.* **2015**, *54* (46), 11592–11609.
- (48) Jana, A. K.; Maiti, D. Assessment of the implementation of vapor recompression technique in batch distillation. *Sep. Purif. Technol.* **2013**, *107*, 1–10.
- (49) Luo, H.; Bildea, C. S.; Kiss, A. A. Novel heat-pump-assisted extractive distillation for bioethanol purification. *Ind. Eng. Chem. Res.* **2015**, *54*, 2208–2213.
- (50) Contreras-Zarazúa, G.; et al. Multi-objective optimization involving cost and control properties in reactive distillation processes to produce diphenyl carbonate. *Comput. Chem. Eng.* **2017**, *105*, 185–196.
- (51) Zhang, Q.; Liu, M.; Zeng, A. Performance enhancement of pressure-swing distillation process by the combined use of vapor recompression and thermal integration. *Comput. Chem. Eng.* **2018**, *120*, 30.
- (52) Guthrie, K. M. Capital cost estimation. *Chem. Eng.* **1969**, *24*, 114–142.
- (53) Turton, R.; Bailie, R. C.; Whiting, W. B.; Shaiwitz, J. A.; Bhattacharyya, D.; *Analysis, Synthesis and design of chemical processes*, 4th ed.; Prentice Hall: 2012.
- (54) Goedkoop, M.; Spriensma, R.; *The Eco-Indicator 99. A Damage Oriented Method for Life Cycle Impact Assessment*; Methodology report nr. 1999/36A; Pré Product Ecology Consultants: 2001.
- (55) Guillen-Gosalbez, G.; Caballero, J. A.; Jimenez, L. Application of life cycle assessment to the structural optimization of process flowsheets. *Ind. Eng. Chem. Res.* **2008**, *47* (3), 777–789.
- (56) Alexander, B.; Barton, G.; Petrie, J.; Romagnoli, J. Process synthesis and optimization tools for environmental design: methodology and structure. *Comput. Chem. Eng.* **2000**, *24* (2–7), 1195–1200.

(57) Quiroz-Ramírez, J. J.; Sánchez-Ramírez, E.; Hernández-Castro, S.; Segovia-Hernández, J. G.; Ponce-Ortega, J. M. Optimal planning of feedstock for butanol production considering economic and environmental aspects. *ACS Sustainable Chem. Eng.* **2017**, *5* (5), 4018–4030.

(58) Mettler, T.; *Der Vergleich von Schutzgütern-Ausgewählte Resultate einer Panelbefragung. tze zum Vergleich von Umweltsch;* ETH Zurich: Switzerland, 1999.

(59) American Institute of Chemical Engineers. *Guidelines for chemical Process Quantitative Risk Analysis*; John Wiley & Sons: New York, NY, USA, 2000.

(60) Crowl, Daniel A.; Louvar, Joseph F. *Chemical process safety: fundamentals with applications*; Pearson Education: 2001.

(61) National Institute for Occupational Safety and Health (NIOSH), <https://www.cdc.gov/niosh/index.htm> (accessed 2018).

(62) Górak, Andrzej; Zarko, Olujic, Eds. *Distillation: equipment and processes*; Academic Press: 2014.

(63) Rangaiah, G. P.; *Stochastic global optimization: Techniques and applications in chemical engineering*; World Scientific: 2010.

(64) Storn, R.; Price, K. Differential evolution—a simple and efficient heuristic for global optimization over continuous spaces. *Journal of Global Optimization* **1997**, *11* (4), 341–359.

(65) Sánchez-Ramírez, E.; Quiroz-Ramírez, J. J.; Segovia-Hernández, J. G.; Hernández, S.; Ponce-Ortega, J. M. Economic and environmental optimization of the biobutanol purification process. *Clean Technol. Environ. Policy* **2016**, *18* (2), 395–411.

(66) Srinivas, M.; Rangaiah, G. P. Differential evolution with TL for solving nonlinear and mixed-integer nonlinear programming problems. *Ind. Eng. Chem. Res.* **2007**, *46*, 7126–7135.

(67) Glover, F. Tabu search—part I. *ORSA. Journal on computing* **1989**, *1* (3), 190–206.

(68) Wang, Z.; Rangaiah, G. P. Application and analysis of methods for selecting an optimal solution from the Pareto-optimal front obtained by multiobjective optimization. *Ind. Eng. Chem. Res.* **2017**, *56* (2), 560–574.

(69) Hernández, S.; Segovia-Hernández, J. G.; Rico-Ramírez, V. Thermodynamically equivalent distillation schemes to the Petlyuk column for ternary mixtures. *Energy* **2006**, *31* (12), 2176–2183.

(70) Yildirim, Ö.; Kiss, A. A.; Kenig, E. Y. Dividing wall columns in chemical process industry: a review on current activities. *Sep. Purif. Technol.* **2011**, *80* (3), 403–417.

(71) Widagdo, S.; Seider, W. D. Azeotropic Distillation. *AIChE J.* **1996**, *42*, 96–130.